

MOLECULAR DYNAMICS AND DIELECTRIC RELAXATION OF HOMOCYSTEINE LAYER BETWEEN GRAPHITE WALLS – COMPUTER SIMULATION

P. Raczyński and Z. Gburski

Institute of Physics, University of Silesia, Uniwersytecka 4, 40-007 Katowice, Poland

Received: December 10, 2009

Abstract. Molecular dynamics (MD) studies are presented for a homocysteine $C_4H_9NO_2S$ layer located between parallel graphite walls. We calculated several dynamical observables of homocysteine at the physiological temperature $T \approx 309K$: the radial distribution function, the mean square displacement, the linear velocity autocorrelation function, the translational diffusion coefficient, the second rank order parameter. Attention was focused on the total dipole moment \vec{M} autocorrelation function $\hat{C}(t) = \langle \vec{M}(t) \cdot \vec{M}(t) \rangle / \langle \vec{M}(0)^2 \rangle$, the dielectric loss spectrum $\epsilon''(\nu)$ and the absorption coefficient $\alpha(\nu)$. A comparison with the dielectric relaxation of a pure homocysteine sample (without a graphite wall) is also presented and discussed.

1. INTRODUCTION

The functions that homocysteine ($C_4H_9NO_2S$) plays in a human body are the subject of the current debate. For example, a high level of blood serum homocysteine is considered to be a marker of a potential cardiovascular (a risk factor for heart attack and stroke) disease. It is not clear yet whether high serum homocysteine itself is a problem or merely an indicator of the existing problems [1-4]. Elevated levels of homocysteine have been linked to increased fractures in elderly persons [5,6]. The molecular level mechanisms for the mentioned and other activities of $C_4H_9NO_2S$ are not fully understood. Knowledge of the properties of homocysteine systems may help, when the role they play in the complex biological environment is considered. In this paper the molecular dynamics (MD) method has been used to study a pure bulk sample of homocysteine as well as a layer of $C_4H_9NO_2S$ molecules located between graphite walls. To our knowledge, no MD simulations of dielectric relaxation of bulk

homocysteine have been reported. The same applies to the homocysteine ensemble in a confined environment, i.e. between graphite walls in our case. The preliminary study reported here might be of some use in a search for new nano- or mezocontainers for homocysteine storage, an issue of importance in molecular medicine [3,4].

2. SIMULATION DETAILS

The standard Lennard-Jones (LJ) interaction potential $V(r_{ij})$ was used between the atoms (sites) of homocysteine [7]. Namely, $V(r_{ij}) = 4\epsilon[(\sigma/r_{ij})^{12} - (\sigma/r_{ij})^6]$, where r_{ij} was the distance between the atoms i th and j th, ϵ was the potential minimum at the distance $2^{1/6}\sigma$, k_B was the Boltzmann constant. The L-J potentials parameters ϵ and σ are given in Table 1 [8-10].

The rigid-body homocysteine molecule contains 17 atomic sites. Homocysteine was treated as rigid a body, since attention was focused on the dynamic of a molecule as a whole, at this stage the internal

Corresponding author: Z. Gburski, e-mail: zgburski@us.edu.pl

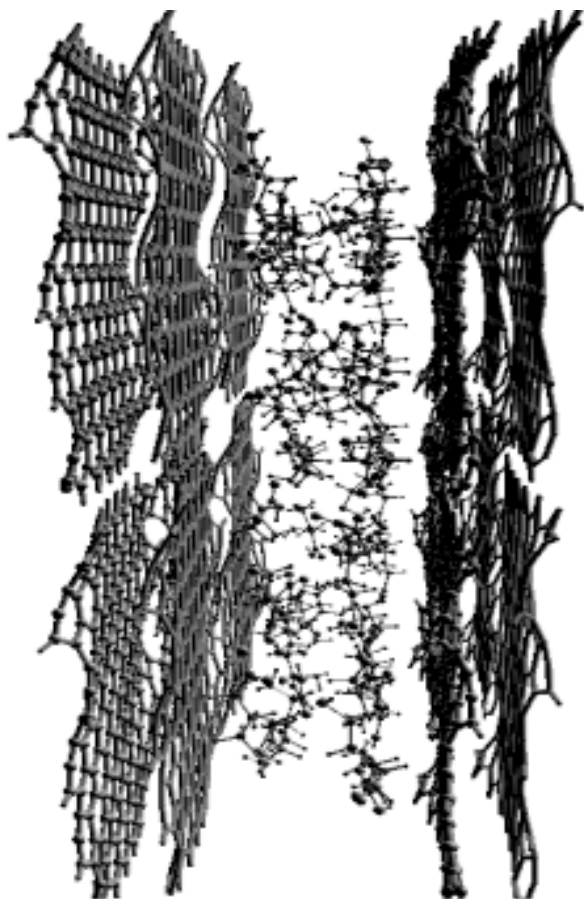


Fig. 1. A snapshot of the instantaneous configuration in case of homocysteine molecules localized between graphite walls.

vibration of atoms inside a molecule was not considered. Moreover, the dipole moments of homocysteine were included by putting the charges $-0.376 e$ on the oxide, $-0.157 e$ on the sulfur, $-0.53 e$ on the nitrogen and $0.376 e$, $0.157 e$, $0.0256 e$, $0.0256 e$ on the bonded hydrogens, obtained from ArgusLab [11].

The L-J potentials parameters between unlike atoms were calculated by the Lorentz-Berthelot rules $\sigma_{A-B} = (\sigma_A + \sigma_B)/2$ and $\epsilon_{A-B} = \sqrt{\epsilon_A \epsilon_B}$ [12,13], where A, B were different atoms. The classical Newton equations of motion were integrated by the predictor-corrector Adams-Moulton algorithm [7]. Our own MD code was used. The integration time step was 0.8 fs which ensured total energy conservation within 0.01% . The total simulation time was 120 ps ($1.5 \cdot 10^5$ time steps). The initial distribution of molecules was generated by the Monte-Carlo (MC) algorithm [7].

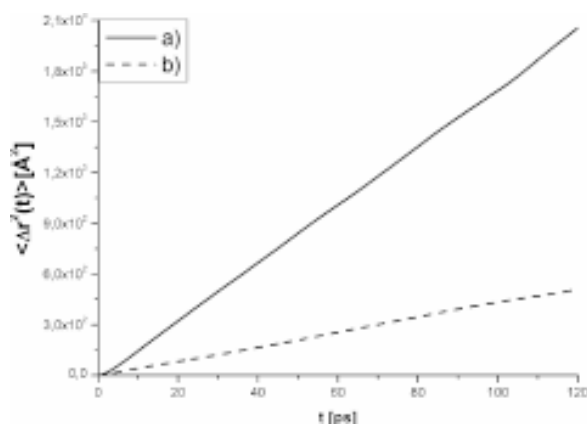


Fig. 2. The mean square displacement of the center of mass of homocysteine in case of: a) bulk sample, b) homocysteine layer at $T = 309\text{K}$.

3. RESULTS

Standard MD simulations for a statistical NVT ensemble with periodic boundary conditions [7] at the constant physiological temperature $T = 309\text{K}$ are made in this paper. The properties of a system composed only of homocysteine molecules (bulk sample) as well as an ensemble of $\text{C}_4\text{H}_9\text{NO}_2\text{S}$ molecules confined between graphite walls are discussed. The separation distance between graphite walls is chosen as 16 \AA , it guarantees that homocysteine molecules “feel” the influence of the graphite walls but still have some space to perform translatory/rotatory motions. An example of an instantaneous configuration of an ensemble of homocysteine molecules between graphite walls at $T = 309\text{K}$ is shown in Fig. 1. The mean square displacement (MSD) $\langle |\Delta \vec{r}(t)|^2 \rangle$ of the center of mass of homocysteine, where $\Delta \vec{r}(t) = \vec{r}(t) - \vec{r}(0)$ and \vec{r} is the position of the center of mass of a single molecule is shown in Fig. 2. It is known from the Einstein relation between MSD and the translational diffusion coefficient D , $\langle |\Delta \vec{r}(t)|^2 \rangle = 6Dt$ [14] that the nonzero slope of $\langle |\Delta \vec{r}(t)|^2 \rangle$ is an indicator of mobility (translational diffusion) of molecules. Fig. 2a shows that it is indeed the case for the bulk homocysteine sample at $T = 309 \text{ K}$. The calculated diffusion coefficient, from the linear part of the slope of $\langle |\Delta \vec{r}(t)|^2 \rangle$, in the bulk system studied at $T \approx 309\text{K}$ is: $2.96 \cdot 10^{-4} \text{ cm}^2/\text{s}$. The lower slope of $\langle |\Delta \vec{r}(t)|^2 \rangle$ for the molecule between the graphite walls (Fig. 2b) means that the walls partly moderate the translational mobility of homocysteines. The reflection of this is a much lower (one order of magnitude) value

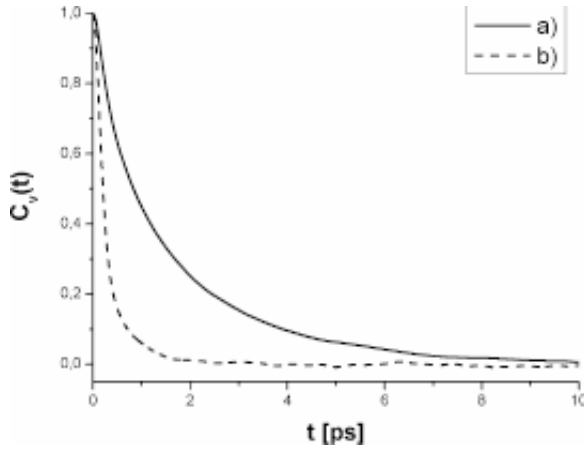


Fig. 3. The linear velocity autocorrelation function of the center of mass of homocysteine in case of: a) bulk sample, b) homocysteine layer at $T = 309\text{K}$.

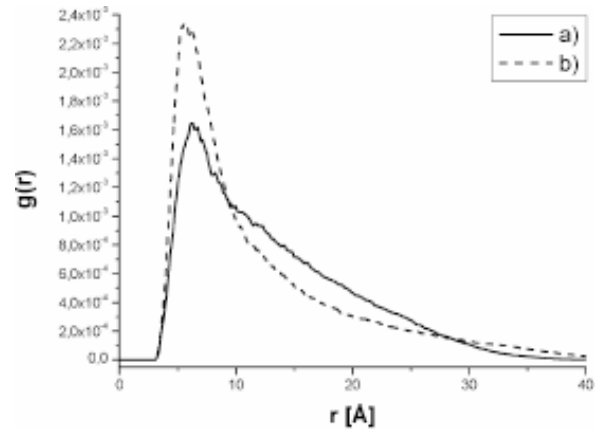


Fig. 4. The radial distribution function of the center of mass of homocysteine in case of: a) bulk sample, b) homocysteine layer at $T = 309\text{K}$.

of the translational diffusion coefficient $D = 7.1 \cdot 10^{-5} \text{ cm}^2/\text{ps}$, comparing to $D = 2.96 \cdot 10^{-4} \text{ cm}^2/\text{ps}$ in case of the bulk sample.

The linear velocity autocorrelation function $C_v(t) = \langle \vec{v}(t) \vec{v}(0) \rangle \cdot \langle \vec{v}(0) \vec{v}(0) \rangle^{-1}$ where $\vec{v}(t)$ is the translational velocity of the homocysteine molecule is shown in Fig. 3. The correlation function $C_v(t)$ for the bulk sample decays almost exponentially $C_v(t) \sim \exp(-t/\tau_v)$. The decorrelation process is therefore quite efficient and governed by the single correlation time $\tau_v = 1.44 \text{ ps}$ obtained by the fitting procedure. The velocity correlation function $C_v(t)$ of the center of mass of the homocysteine in the layer (Fig. 3b) decays exponentially ($\tau_v = 0.29 \text{ ps}$), much faster than in case of the bulk sample. This shows that the graphite walls quite strongly enhance the velocity decorrelation process. In addition to the homocysteine-homocysteine collisions it is also interactions with the walls that decorrelate the velocity. The calculated radial distribution function $g(r)$ of the center of mass of the homocysteine in the layer and the pure bulk sample is presented in Fig. 4. The lack of sharp peaks of $g(r)$ for bulk sample indicates that this sample is not in a solid phase. The graphite walls force a little closer and more regular packing of homocysteines. The majority of molecules choose the mean distance $d = 5.3 \text{ Å}$ to the near neighbors, comparing to $d = 6.2 \text{ Å}$ for the bulk sample. The number of molecules which occupy the mean near neighbor distance is much higher in case of confined homocysteine. We have also calculated the second-rank orientational order parameter $P_2 = \langle 3\cos\theta_i \cos\theta_j + \delta_{ij} \rangle / 2$ where $i, j = x, y, z$ are

indices referring to the laboratory frame. The brackets $\langle \rangle$ represent thermal averaging (over the whole sample and simulation time). θ is the angle between the molecular long axis and the eigenvector of the order tensor P_2 corresponding to the maximum eigenvalue [16]. The parameter, P_2 , should be zero in case of a completely isotropic liquid. In our case, the value of P_2 increases twice while passing from a bulk sample ($P_2 = 0.12$) to a homocysteine layer ($P_2 = 0.25$). It means that the interaction between carbon atoms of graphite walls and homocysteine stimulates and enhances partial ordering in the homocysteine layer.

The normalized total dipole moment correlation function $\hat{C}(t) = \langle \vec{M}(t) \cdot \vec{M}(t) \rangle / \langle \vec{M}(0)^2 \rangle$, where $\vec{M} = \sum_{i=1}^n \vec{\mu}_i$ and $\vec{\mu}_i$ is the dipole moment of i -th homocysteine is presented in Fig. 5. The correlation function $\hat{C}(t)$ of bulk sample decays almost exponentially (typical Debye relaxation) with the correlation time $\tau \approx 1.55 \text{ ps}$. It can be seen from Fig. 5 that the normalized total dipole moment correlation function $\varepsilon''(\nu)$ decays much slower while the homocysteine molecules are placed between the graphite walls. The correlation time τ is equal to $\approx 8.07 \text{ ps}$, comparing to $\tau \approx 1.55 \text{ ps}$ of the bulk sample. Due to the high orientational disorder in the bulk sample, its total dipole moment relaxes more randomly leading to a faster dielectric relaxation. On the contrary, the total dipole moment relaxation becomes slower in the layer where the orientational order is substantially higher. In a dielectric experiment it is the frequency dependence of the dielectric loss $\varepsilon''(\nu)$ that is measured which is the imaginary part of com-

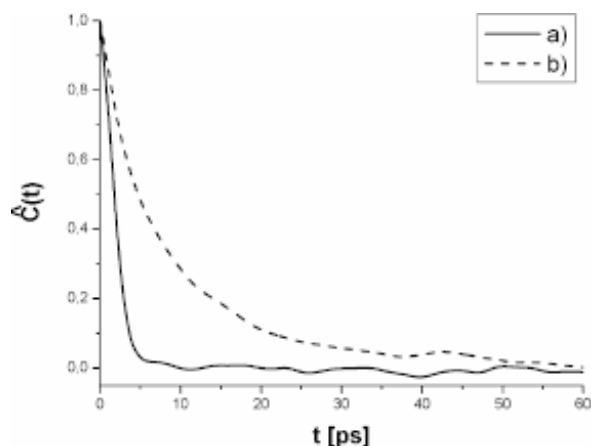


Fig. 5. The total dipole moment autocorrelation function of homocysteine in case of: a) bulk sample, b) homocysteine layer at $T = 309\text{K}$.

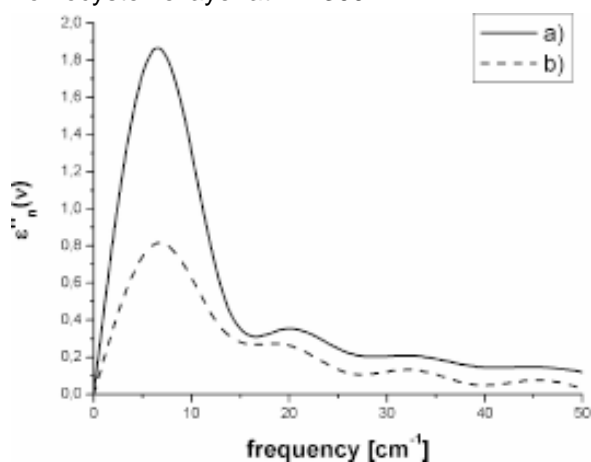


Fig. 6. The normalized dielectric loss of homocysteine in case of: a) bulk sample, b) homocysteine layer at $T = 309\text{K}$.

plex dielectric permittivity $\epsilon^*(\nu) = \epsilon'(\nu) - i\epsilon''(\nu)$ [15], $i = \sqrt{-1}$. In case of pure dipolar absorption and in the classical limit ($\eta \rightarrow 0$) $\epsilon''(\nu)$ is related to the cosine Fourier transform of $C(t) = \langle \vec{M}(t) \cdot \vec{M}(t) \rangle$. Fig. 6 shows the normalized dielectric loss $\epsilon''_n(\nu) = \nu \int_0^\infty dt \hat{C}(t) \cos(2\pi\nu t)$ of the studied sample. A less ordered structure of the bulk sample comparing to the layer has been already pointed out in $g(r)$ plot (see Fig. 4). Consequently, the peak of the dielectric loss $\epsilon''_n(\nu)$ of the bulk sample prevails its counterpart of the layer, see Fig. 5. The frequency ν_{\max} of a maximum of $\epsilon''_n(\nu)$ is $\nu_{\max} = 1.95 \cdot 10^{11}$ Hz. The normalized absorption coefficient $\alpha_n(\nu)$ is presented in Fig. 6 for both the studied systems. Fig. 7 shows that the maximum dielectric absorption should be expected around 195 GHz. As far as we know, no experimental report on the dielectric absorption of a

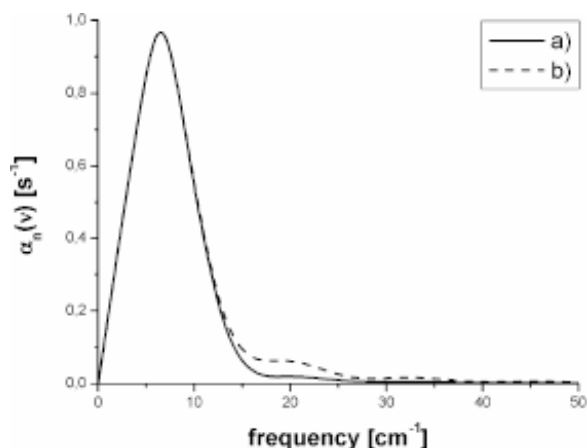


Fig. 7. The normalized absorption coefficient of homocysteine in case of: a) bulk sample, b) homocysteine layer at $T = 309\text{K}$.

Table 1. Lennard – Jones potential parameters.

| Atoms | σ/k_B [K] | σ [Å] | m [10^{-25} kg] |
|-------|------------------|--------------|----------------------|
| C | 58.2 | 3.85 | 0.2 |
| O | 88.7 | 2.95 | 0.27 |
| N | 53.22 | 3.49 | 0.12 |
| S | 209.76 | 3.6 | 0.53 |
| H | 12.4 | 2.81 | 0.02 |

bulk homocysteine or homocysteine layer has been announced to date.

4. CONCLUSION

We have shown that both homocysteine systems studied are not in a solid phase at the physiological temperature $T = 309\text{K}$. Nevertheless, the properties of bulk and confined homocysteine samples differ significantly. The molecules $\text{C}_4\text{H}_9\text{NO}_2\text{S}$ exhibit higher mobility when in a bulk sample (unconfined). The confined environment (graphite walls) enhances an orientational ordering of molecules, partly limiting their rotational freedom in this way. A consequence of this is substantially slower dielectric relaxation of homocysteines confined in a layer between graphite walls. The simulated dielectric spectra, dielectric correlation times, linear velocity autocorrelation function, velocity correlation times, and diffusion coefficients are reported for the first time both for the confined and unconfined samples of homocysteine. The frequency of a maximum of the dielectric loss $\epsilon''_n(\nu)$ of a homocysteine sample around $\nu_{\max} = 1.95 \cdot 10^{11}$ Hz is predicted, and this may serve as a guideline for future „real life” experiments. The pre-

liminary study reported here might be of some use in a search for new nano- or mezocontainers for homocysteine storage, an issue of importance in molecular medicine.

REFERENCES

- [1] J. Selhub // *Annual Review of Nutrition* **19** (1999) 217.
- [2] J. W. Miller, M. R. Nadeau, D. Smith and J. Selhub // *American Journal of Clinical Nutrition* **59** (1994) 1033.
- [3] C. Stehouwer and C. van Guldener // *Expert Opinion on Pharmacotherapy* **2** (2001) 1449.
- [4] S. Zoungas, B.P. McGrath, P. Branley, P.G. Ker, C. Muske, R. Wolfe, R.C. Atkins, K. Nicholls, M. Fraenkel, B.G. Hutchison, R. Walker and J.J. McNeil // *J. Am. Coll. Cardiol.* **47** (2006) 1108.
- [5] J. B. van Meurs // *New England Journal of Medicine* **350** (2004) 2033.
- [6] R. R. McLean // *New England Journal of Medicine* **350** (2004) 2042.
- [7] M. P. Allen and D. J. Tildesley, *Computer simulation of liquids* (Oxford University Press, Oxford, 1989).
- [8] X. Daura, A. E. Mark and W. F. van Gunsteren // *Journal of Computational Chemistry* **19** (1998) 535.
- [9] Thomas la Cour Jansen, *Theoretical Simulation of Nonlinear Spectroscopy in the Liquid Phase* (PH.D. thesis, 2002).
- [10] T. Kuznetsova and B. Kvamme // *Energy Conversion and Management* **43** (2002) 2601.
- [11] <http://www.planaria-software.com/> and citations therein.
- [12] D. Frenkel and B. Smith, *Understanding molecular simulation* (Academic Press, New York, 2002).
- [13] D. C. Rapaport, *The art of molecular dynamics simulation* (Cambridge University Press, Cambridge, 1995).
- [14] J. P. Hansen and I. McDonald, *Theory of Simple Liquid* (Academic Press, London, 1986).
- [15] C. L. F. Böttcher and P. Bordewijk, *Theory of dielectric polarization* (Elsevier, Amsterdam, 1995).
- [16] P. G. de Gennes, *The Physics of Liquid Crystals* (Clarendon, Oxford, 1974).